

ON-CHIP DOUBLE EMULSION DROPLET ASSEMBLY USING ELECTROWETTING-ON-DIELECTRIC AND DIELECTROPHORESIS

W. WANG,^a T. B. JONES,^{a*} and D. R. HARDING^b

^aUniversity of Rochester, Department of Electrical and Computer Engineering, Rochester, New York 14627

^bUniversity of Rochester, Department of Chemical Engineering, Rochester, New York 14627

Received April 2, 2010

Accepted for Publication July 1, 2010

The double emulsion (DE) droplets used for fabrication of cryogenic foam targets for inertial confinement fusion experiments require precisely controlled volumes. On-chip electric field actuated microfluidic assembly of DE droplets can be used to achieve such precision. The electrowetting-on-dielectric and dielectrophoresis effects make it possible to manipulate both conductive and dielectric droplets simultaneously on a substrate. Aqueous and nonaqueous liquid droplets precisely dispensed from two reservoirs on a microfluidic chip are trans-

ported and combined to form oil-in-water-in-air or water-in-oil-in-air DE droplets. The dispensing reproducibility is studied as a function of a set of operation parameters. Conditions for spontaneous emulsification for DE formation are developed in terms of droplet surface energies.

KEYWORDS: double emulsion droplet, electrowetting-on-dielectric, dielectrophoresis

Note: Some figures in this paper are in color only in the electronic version.

I. INTRODUCTION

Inertial confinement fusion experiments use spherical organic polymer shells as mandrels for cryogenic foam targets. The targets are typically fabricated by polymerizing double emulsion (DE) shells and then voiding the inner fluids.^{1,2} In this process, special care has to be taken to assure DE droplet size uniformity because fusion experiments impose rigid requirements upon the sphericity and wall thickness uniformity of foam targets.

Up to the present, the formation of uniform DE droplets has relied mainly on the controlled merging of two immiscible fluids.¹⁻⁵ Current preparation of DE droplets for target fabrication is done using a triple-orifice droplet generator.¹ Two concentric orifices are inserted into a tube where there is a flow of an exterior oil phase. An interior oil phase droplet is surrounded by a water phase shell, and they are pinched off at the tips of the two concentric orifices by the exterior oil flow to form oil-in-water-in-oil DE droplets in the tube. This preparation method generates remarkably monodisperse emulsions

with good uniformity. However, the DE droplet size is severely constricted by the device dimensions. In this paper, we propose a DE assembly line based on a “lab-on-a-chip” droplet generator, where individual water and oil droplets generated from an on-chip dispensing system are combined directly to form DEs. As an entirely voltage-controlled microfluidic system, this scheme has the advantages of reconfigurability, flexibility, and scalability.

II. BACKGROUND

We form “droplet within a droplet” systems in air. While these are not real DEs, they can be dispersed in an immiscible continuous phase to form DEs as required for target fabrication operations. Because the formation of emulsion droplets in air requires combining at least one water droplet and one oil liquid droplet, we use electrowetting-on-dielectric (EWOD) and dielectrophoresis (DEP) simultaneously to dispense and transport water and oil droplets, respectively. Because all actuation is electrical, we can program each step and thus obtain maximum operational flexibility.

*E-mail: Jones@ece.rochester.edu

II.A. Electrowetting-on-Dielectric

The electrowetting effect describes the observable influence of an electric field on both bulk liquid motions and the contact angle. The motive force is due to the response of the free electric surface charge to the electric field.⁶⁻⁸ In an EWOD-based microfluidic device as shown in Fig. 1, droplets are sandwiched between parallel plates and are manipulated by applying voltages to a series of adjacent electrodes on the bottom. A wide variety of fundamental fluid operations has been realized using EWOD. These operations include droplet transport,⁹ dispensing,¹⁰⁻¹² separation,^{10,12} coalescence,¹⁰ dilution,¹³ and others.

II.B. Dielectrophoresis

The DEP force is the force exerted on dielectrics when subjected to a nonuniform electric field.^{14,15} As another extensively studied mechanism for droplet manipulation, DEP is useful for manipulation of insulating, polarizable media. For example, decane cannot be moved by EWOD (Ref. 16), but can be moved by DEP (Ref. 17).

EWOD and DEP are two observable effects of liquid under electrostatic fields, both of which are electromechanical in nature. Jones⁷ first clarified the frequency-dependent relationship between these two mechanisms. For a liquid with finite electrical conductivity and dielectric constant, there exists a critical frequency that separates conductive (EWOD) and dielectric (DEP) behavior.^{7,18,19} At high frequencies the electric field lines penetrate the liquid, so that the electromechanical response of liquid at high frequency is equivalent to the case of an insulating liquid and is the same as liquid DEP.

II.C. General Microfluidic Platform Based on EWOD and DEP

The combination of droplet-based EWOD and DEP microfluidics makes it possible to manipulate both conductive and insulating droplets on the same chip. Conceptually, such a combination of EWOD and DEP may be visualized with the parallel-plate scheme shown in

Fig. 1. The device consists of two parallel glass plates: a bottom plate, which consists of a patterned array of individually addressable electrodes, and a top plate, which is a continuous ground electrode. Usually, the bottom plate is coated with a dielectric layer, and both the top and bottom surfaces are covered with a thin hydrophobic film to decrease the surface wettability.

III. MICROFABRICATION AND EXPERIMENTS

The basic features of the droplet-based microfluidic system are illustrated in a cross-sectional view in Fig. 1. The bottom glass substrate is evaporatively coated with 100 nm of aluminum and then photolithographically patterned into a two-dimensional electrode array. The structure is then spin-coated with 0.5 μm of spin-on-glass (Futurrex IC1-200) as the dielectric layer and 1 μm of amorphous fluoropolymer (DuPont Teflon-AF) as a hydrophobic coating. The top plate is a glass plate with a transparent ITO layer as a ground electrode covered by 1 μm of Teflon-AF as a hydrophobic coating.

The top substrate is positioned above the bottom substrate by appropriate spacers. Voltages applied to individual electrodes are controlled by a LabView-based controller. It is important to recognize that different voltages are applied for EWOD actuation and DEP actuation. For EWOD actuation, direct-current (dc) or low-frequency alternating-current (ac) voltage, typically <100 V, is employed. For oil DEP actuation, dc or ac voltage (50 Hz to 100 000 Hz) is used, but usually >250 V. The droplet volumes are determined by image analysis using a Matlab routine.

IV. DROPLET DISPENSING REPRODUCIBILITY

In a typical dispensing operation, a liquid finger is drawn from a large reservoir droplet. Liquid pinch-off occurs by activating the electrode at the front end of the liquid finger and the reservoir electrode and by deactivating the electrodes in between (the cutting electrode) until the

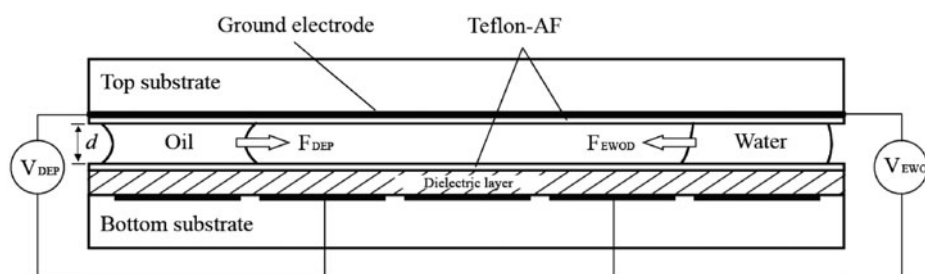


Fig. 1. Cross section of a parallel-plate device containing a dielectric layer on the bottom plate to manipulate oil and water droplets by DEP and EWOD, respectively.

liquid front is separated from the liquid bulk. Successful pinch-off requires an application of electrode voltages above some threshold value to establish the required internal pressure differences between the liquid in the reservoir and the cutting point.⁶ The sequence of steps for droplet dispensing is shown in Fig. 2. EWOD-based water droplet dispensing has been widely studied,^{10–12} but dielectric droplet (oil) dispensing has not received much attention. Here we demonstrate repeatable dielectric droplet dispensing on a microfluidic chip as shown in Fig. 2. Because of the difference in the electric actuation mechanism, oil droplet manipulation by DEP requires much higher voltages than EWOD dispensing of aqueous droplets.

Dispensing reproducibility is of paramount importance in laser target fabrication because the uniformity of subsequently formed DE droplets is largely determined by controlling the initial liquid volume. The requirements for DE droplet uniformity are described in the Appendix. It has been observed that the dispensed drop volume is usually somewhat larger than the volume subtended by a square electrode (volume = a^2d , where a is the length of a square electrode in the electrode array and d is the spacing between the bottom and top substrates).¹² The reason is that a liquid tail formed after separation adds some additional liquid to the already formed droplet. It is this volume that causes the variability in the dispensing operation. In this research we investigated the effects of applied voltage and electrode shape on droplet volume control for an on-chip dispensing system because they both directly impact the tail volume.

IV.A. Effect of Applied Voltage on Droplet Volume Variation

We investigated the dependence of dispensed water drop volume upon the actuation voltage in a structure

with 1-mm square electrodes. The droplet volume becomes sensitive when the applied voltage is close to the minimum required value for pinch-off. For example, when the applied voltage decreased from 62.5 V to the minimum pinch-off voltage of 55.0 V, the droplet volume dropped by almost 30%, as shown in Fig. 3. The same result is observed with both square and circular dispensing electrodes. This voltage dependence is a result of the effect on the tail shapes during pinch-off. As shown in Fig. 4, a smaller tail is observed at lower voltage, and the pinch-off position also moves more closely toward the individual droplet. The shape of the tail changes because the liquid finger necking depends on the electrowetting force, which is directly related to applied voltage.⁶

Figures 4c and 4g show that with square electrodes, a smaller area of the dispensing electrode is filled by liquid during pinch-off at lower voltage than at higher voltage. This smaller finger front may also contribute to reduced dispensed droplet volume. No obvious change in the finger front is observed for circular electrode structures, as shown in Figs. 4d and 4h, but the droplet volume remains very sensitive to voltage change. In general, the liquid tail plays the most important role in determining droplet volume variation.

IV.B. Effect of Cutting Electrode on Droplet Volume and Reproducibility

We tested electrode structures with different cutting electrode lengths L to investigate the effect of this parameter on droplet volume and reproducibility. As shown in Fig. 5, the dispensed droplet volume increases directly with L . Droplets with average volumes of 103 and 183 nL were dispensed on a 1- × 1-mm square electrode using cutting electrodes of lengths $L = 2$ and 3 mm, respectively. These

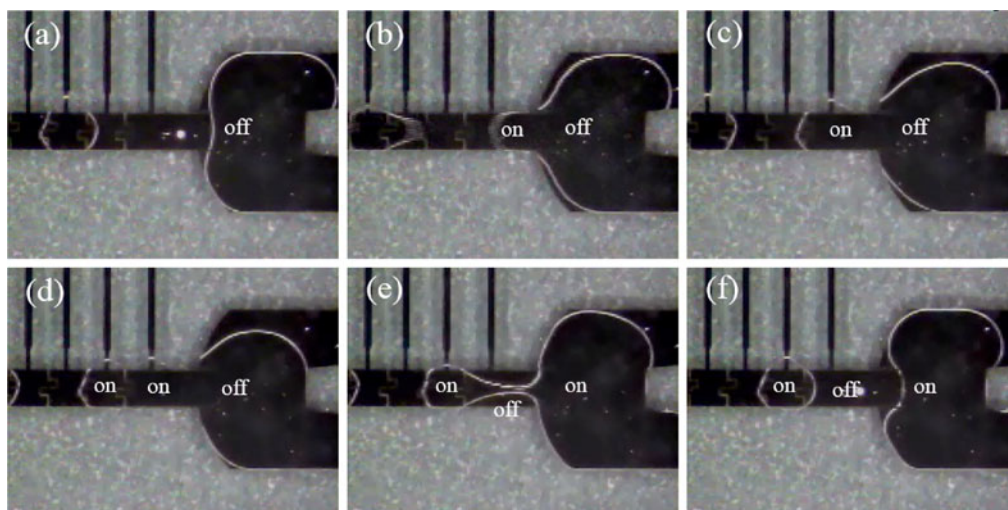


Fig. 2. Top view of an on-chip dispenser showing the sequence of a silicone oil droplet being formed. (a) The reservoir and an already-formed droplet. (b, c, d) The liquid finger is formed, and meanwhile the first droplet is delivered away. (e) The pinch-off occurs. (f) A new droplet is formed.

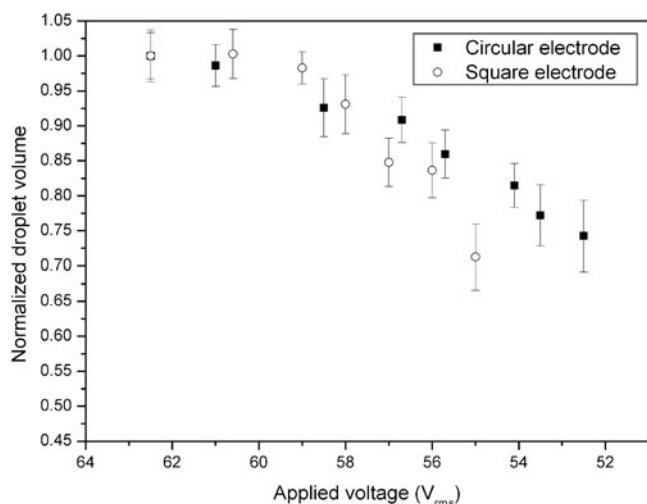


Fig. 3. The normalized (normalize to the droplet volume at 62.5 V) volume variation of a series of droplets generated by different applied voltages. All tests were done with deionized water. The gap between top and bottom substrates was 85 μm , and the voltage applied was 100-Hz ac.

droplet volumes are greater than the volume subtended by one electrode: 85 nL. The increase in droplet volume is due to the larger tail formed upon longer cutting electrodes during pinch-off. Similar behavior is also observed on 2- \times 2-mm square electrodes.

Droplet volume reproducibility suffers as L is increased. As indicated in Fig. 5 and Table I, the coefficient of variation ($CV = \text{standard deviation}/\text{mean} \times 100\%$) increases significantly when the ratio of the cutting electrode length to standard electrode length L/a approaches $L/a = 3$. This behavior is due to the reduced influence of the cutting electrode on the radius of curvature in the pinch-off region. In fact, the pinch-off position becomes indeterminate for sufficiently large L/a . Large droplet volume variation ($CV = 40\%$) is observed when $L/a = 3$ on a 2- \times 2-mm electrode due to the instability of the pinch-off position; see Fig. 6.

The best reproducibility ($CV = 3.0\%$) is achieved for a cutting electrode of the same length as that of the standard electrodes. This reproducibility is adequate for laser target fabrication (see the Appendix for detailed discussion).

V. ON-CHIP DE FORMATION

V.A. Gibbs Free Energy Model

When two immiscible droplets are brought together, a DE droplet forms spontaneously if the Gibbs free energy is reduced by the emulsification process. The Gibbs

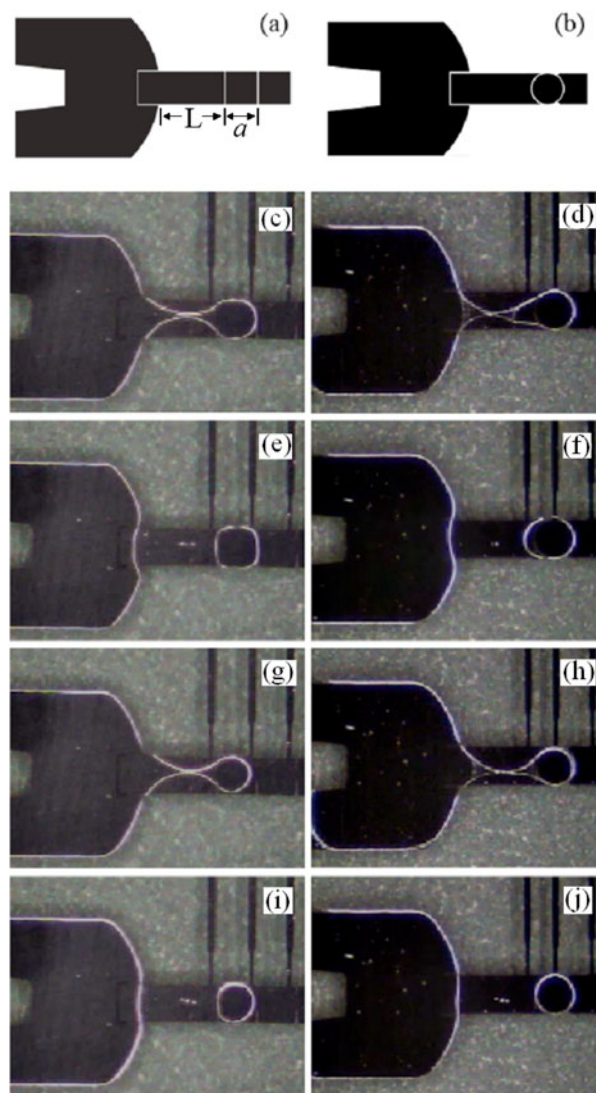


Fig. 4. The effect of applied voltage on droplet volume variation. (a, b) Square and circular dispensing electrodes used for the dispensing experiments. The square electrode is 1 \times 1 mm, and the diameter of the circular electrode is 1 mm. The length of the cutting electrode is 2 mm. (c, e) Pinch-off and the formed droplet on the square electrode by applying 62.5 V_{rms} , 100-Hz ac voltage. (g, i) Pinch-off and the formed droplet on the square electrode by applying 55 V_{rms} , 100-Hz ac voltage. (d, f) Pinch-off and the formed droplet on the circular electrode by applying 62.5 V_{rms} , 100-Hz ac voltage. (h, j) Pinch-off and the formed droplet on the circular electrode by applying 52.5 V_{rms} , 100-Hz ac voltage. In all cases, the gap between the top and bottom substrates is 85 μm .

interfacial energy change between the initial and final states of a DE formation process is

$$\Delta G = G_{DE} - (G_{water} + G_{oil}), \quad (1)$$

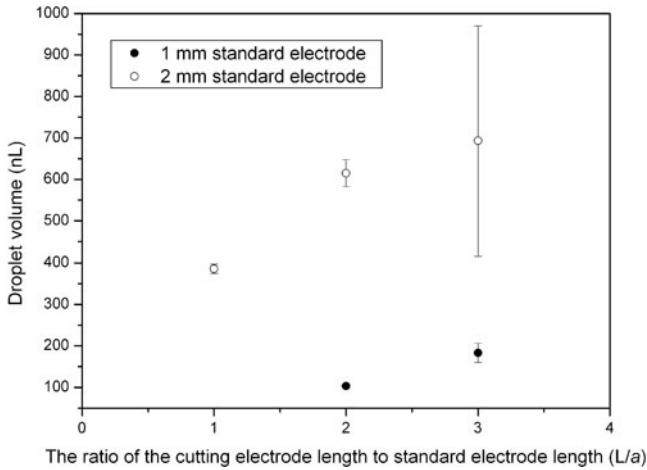


Fig. 5. Average droplet volume versus cutting electrode length. All tests were performed with deionized water. The gap between the top and bottom substrates was 85 μm, and the voltage applied was 90 V_{rms}, 100-Hz ac.

TABLE I

Effect of Cutting Electrode Length on Volume Reproducibility for Droplets Dispensed on 1- and 2-mm Dispensing Electrodes and an 85-μm Channel Gap*

| Electrode Size | L/a = 1 | L/a = 2 | L/a = 3 |
|----------------|---------|---------|---------|
| 1 × 1 mm | | 4.7% | 12.7% |
| 2 × 2 mm | 3.0% | 5.3% | 40% |

*In all cases, the voltage applied was 90 V_{rms}, 100-Hz, ac.

where

G_{DE} = total Gibbs interfacial energy of a DE droplet

G_{water}, G_{oil} = Gibbs surface energies of the individual water and oil droplets forming that DE droplet, respectively.

The Gibbs energy change ΔG is a convenient criterion for testing the likelihood of DE formation. A negative ΔG means the DE formation is favored. In the following, we develop a simple model to calculate the Gibbs surface energy changes associated with DE formation.

The Gibbs surface energy is a sum of the product of interfacial tensions and corresponding surface areas. The surface shape of a droplet sandwiched between parallel plates is strongly affected by the contact angle against the substrate and the spacing between the top and bottom substrates. For the geometry model shown in Fig. 7, the droplet volume is

$$V = 2 \int_0^h \pi x^2 dz$$

$$= 2\pi[(x_0^2 + R^2)h - \frac{1}{3}h^3 + 2x_0R^2(\frac{1}{2}\theta_0 + \frac{1}{4}\sin 2\theta_0)] , \quad (2)$$

where

$$\theta_0 = \theta - \pi/2$$

θ = contact angle on a hydrophobic surface ($\theta > 90$ deg)

$$R = -h/\cos \theta$$

and the spacing between substrates is $2h$.

The lateral surface area and base areas are then

$$S_L = 2 \int_0^{\theta_0} 2\pi(x_0 + R \cos \theta')R d\theta'$$

$$= 4\pi R(x_0\theta_0 + R \sin \theta_0) \quad (3)$$

and

$$S_B = 2\pi(x_0 + R \cos \theta_0)^2 . \quad (4)$$

When $\theta < 90$ deg, droplet volume and droplet surfaces can be derived as

$$V = 2\pi[(x_0^2 + R^2)h - \frac{1}{3}h^3 - 2x_0R^2(\frac{1}{2}\theta_0 + \frac{1}{4}\sin 2\theta_0)] , \quad (5)$$

$$S_L = 2 \int_0^{\theta_0} 2\pi(x_0 - R \cos \theta')R d\theta'$$

$$= 4\pi R(x_0\theta_0 - R \sin \theta_0) , \quad (6)$$

and

$$S_B = 2\pi(x_0 - R \cos \theta_0)^2 , \quad (7)$$

where

$$\theta_0 = \pi/2 - \theta$$

and

$$R = h/\cos \theta .$$

Several studies^{20,21} have reported that for a water-in-oil DE droplet in the parallel-plate structure, the oil becomes entrapped underneath the inner water droplet as illustrated in Fig. 8b. We analyzed the Gibbs surface energy change for both cases of the water droplet directly in contact with the Teflon surface and enclosed by a thin layer of oil. Using Eqs. (2) through (7) and the interfacial tension data shown in Table II, we calculate ΔG for water-in-silicone oil (20 cSt) DE for the configurations of Figs. 8a and 8b. The ΔG per unit total liquid volume is expressed as the ratio of the volume of water to the total

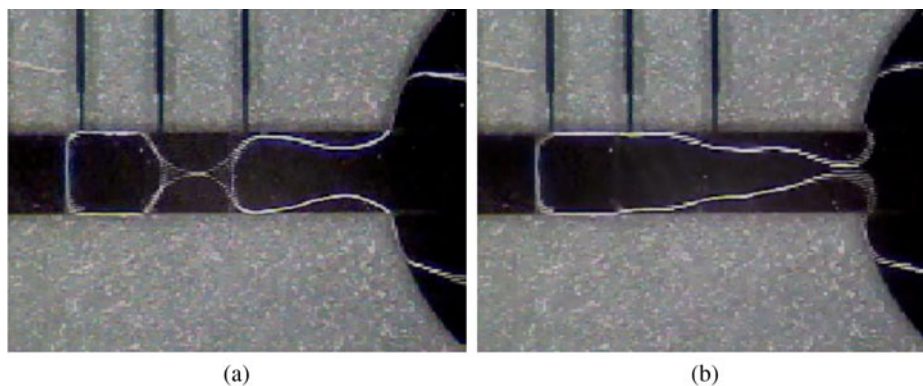


Fig. 6. Instability of the pinch-off position for droplet dispensing on 2-mm standard electrode and a 6-mm cutting electrode. The gap between the top and bottom substrates was $85 \mu\text{m}$, and the voltage applied was $90 V_{\text{rms}}$, 100-Hz ac.

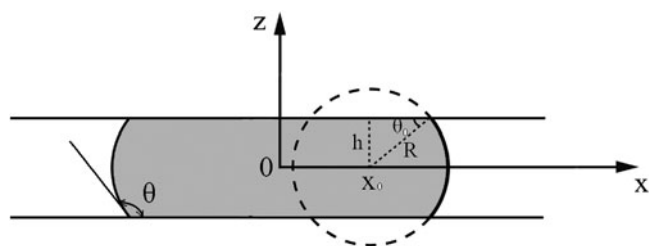


Fig. 7. Droplet geometry when sandwiched between parallel plates.

volume of water and oil in the DE. Both configurations give $\Delta G < 0$, but the configuration with the oil entrapped underneath the water system is energetically favored.

As noted above, a water droplet and an oil droplet usually combine to form a water-in-oil DE because water has a higher surface tension than most oils. But, we can reverse this tendency if we add surfactant Silwet L-77 to the water. The addition of surfactant reduces the effective surface tension of water so that it becomes possible to form oil-in-water DEs. The surface tension for Silwet-treated water (at the surfactant concentration of 0.0625 wt%, listed in Table II) is greater than silicone oil but lower than mineral oil. Therefore, it is not effective to choose silicone oil for oil-in-water DEs. Instead, we chose mineral oil and then calculated ΔG for mineral oil-in-Silwet-treated water as a function of the volume ratio of mineral oil. As shown in Fig. 9, the requirement for DE formation, $\Delta G < 0$, is met. There are also two possible configurations for the oil-in-water DE droplet: The oil droplet rests on the Teflon surface and on a thin layer of water. We calculated ΔG for both cases. Figure 9 shows that the energy is minimized when the inner oil droplet is separated from the Teflon surface by a layer of water. We have some evidence for the existence of this configuration, but further experimental verification is needed.

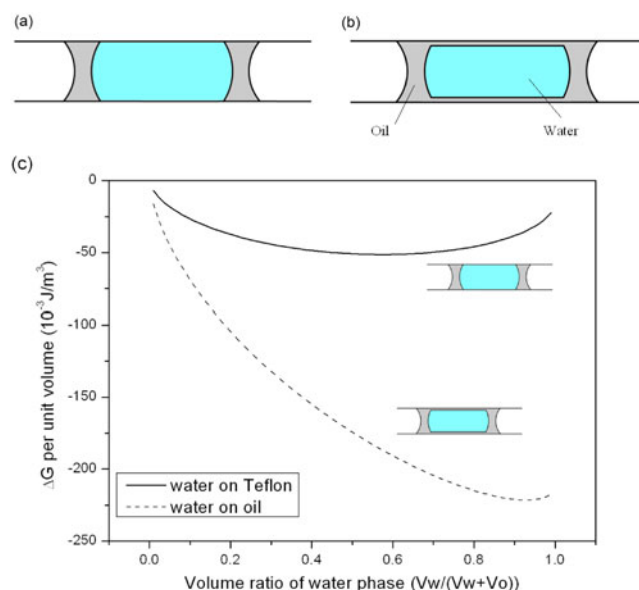


Fig. 8. Water-in-silicone oil (20 cSt) DE droplet in the parallel-plate structure. (a) The inner water droplet rests on the Teflon surface. (b) The inner water droplet rests on a thin layer of oil. (c) ΔG of DE formation for both the cases of (a) and (b).

V.B. Experiments for Water-in-Oil DE Formation

We tested the electric-field actuated formation of water-in-silicone oil DE as shown in Fig. 10. Two silicone oil droplets were first dispensed from the left reservoir through DEP by applying $330 V_{\text{rms}}$, 100-Hz ac voltage on the lower array of electrodes. Then, two de-ionized water droplets were dispensed from the right reservoir through EWOD actuation by application of $85 V_{\text{rms}}$, 100-Hz ac voltage on the upper array of electrodes. With the same EWOD actuation voltages, the water droplets were then transported toward the oil droplets as shown in

TABLE II
Interfacial Tension Data at Room Temperature*

| Interface | Interfacial Tension |
|------------------------------------|---------------------|
| Water/air | 74 |
| Silicone oil (20 cSt)/air | 20.6 ^a |
| Mineral oil/air | 28.1 |
| Silicone oil (20 cSt)/water | 35 ^b |
| Mineral oil/water | 49 ^c |
| Water/Teflon | 49 ^d |
| Silicone oil (20 cSt)/Teflon | 5.6 ^d |
| Mineral oil/Teflon | 10.25 ^d |
| Teflon/air | 18 |
| W _{S-t} ^e /air | 24.7 ^f |
| Mineral oil/W _{S-t} | 4.5 ^b |
| W _{S-t} /Teflon | 2.46 ^d |

*In units of mN/m.

^aDow Corning 200[®] Fluid data sheet.

^bInterfacial tension was determined using an Easy Dye tensiometer.

^cReference 23.

^dInterfacial tension was calculated from Young's equation.

^eW_{S-t} = Silwet-treated water (0.0625 wt%).

^fReference 22.

Figs. 10c and 10d. After the water droplets touched the oil droplets, they were engulfed by the oil droplets to form DE droplets. Furthermore, the water droplets were able to pull the whole merged water-in-oil DE droplets by low-voltage EWOD transport.

V.C. Experiments for Oil-in-Water DE Formation

We performed dispensing experiments with Silwet-treated water solutions at five widely ranging concentrations: 0.00625, 0.0125, 0.025, 0.0625, and 0.125 wt%. Only the 0.00625 wt% Silwet solution could be dispensed smoothly. All the others formed a remarkably persistent "tether" during the pinch-off process. As shown in Fig. 11a, the thin liquid tether is formed between the reservoir and the droplet, preventing its separation. A full understanding of the tether formation in air is still lacking, but similar experiments in oil medium show that surfactant-treated water can be successfully dispensed without tether formation.^{11,12}

One way to break the tether is to use a second liquid finger to disturb it. This mechanism is shown in Fig. 11. The secondary liquid used was pure deionized water. When the pure water finger touches the tether, the Silwet solution in the contact area is diluted locally, and the tether breaks because of the increased surface tension. The entire tether disintegrates into many satellite droplets because of hydrodynamic instability. See Fig. 11d.

This method does not work when the Silwet concentration exceeds 0.125 wt%, in which case the second

water finger seems to mix with the tether instead of breaking it. Apparently, the local dilution is not sufficient to increase the surface tension when the Silwet concentration is far above the critical micelle concentration. Another problem with the tether formed during dispensing is that the electrode shape loses some of its influence in defining the pinch-off curvature, resulting in poor volume reproducibility.

V.D. Other Possible Solutions to the Tether Problem

A second method to avoid the tether is by taking advantage of the pH effect on spreading of Silwet solutions. Radulovic et al.²² found that the wetting ability of Silwet solutions is drastically reduced with the addition of acetic acid, possibly due to the polarization of the trisiloxane head. We also found in experiments that the Silwet surfactant could be strongly affected by the addition of other acids (such as HCl) or bases (such as KOH), and the change in wetting ability by the pH effect is reversible by neutralization. In our work, we have demonstrated that the addition of acid to Silwet-treated water can avoid the tether formation. Then, the dispensed droplet is neutralized by mixing with another base droplet. In this way, the required low surface tension is recovered. The droplet now containing some salts can be used for oil-in-water DEs. The problem with this method is that the reversal process using a base solution takes a long time, typically >1 h. This waiting time would be a major disadvantage for mass production of DE droplets. Also, evaporation of water during such a long period must be prevented.

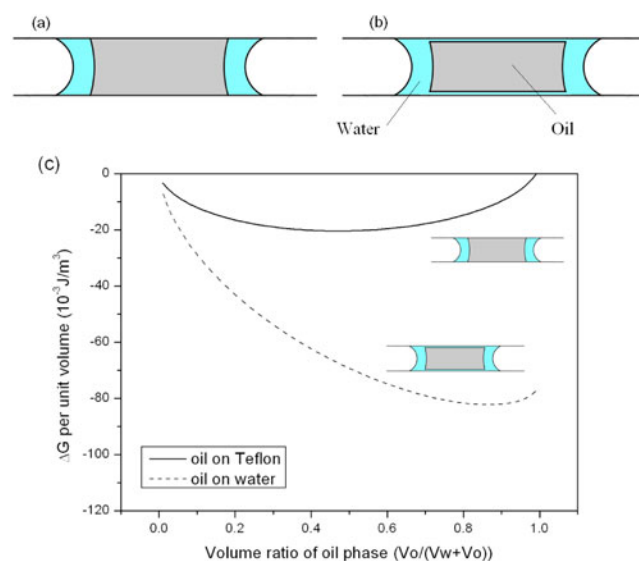


Fig. 9. Mineral oil-in-Silwet-treated water DE formation in parallel plates. (a) The inner oil droplet rests on the Teflon surface. (b) The inner oil droplet rests on a thin layer of water. (c) ΔG of DE formation for both the cases of (a) and (b).

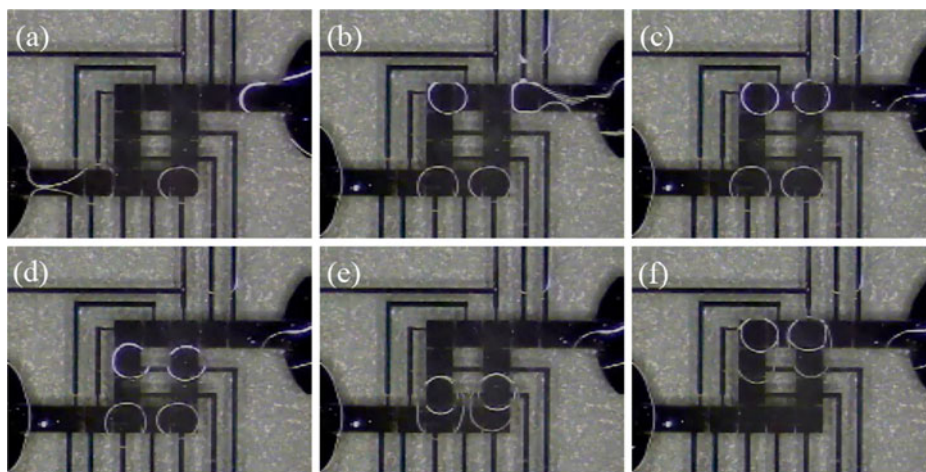


Fig. 10. The formation of water-in-silicone oil DE droplets. (a) Two silicone oil droplets are dispensed through DEP actuation by applying $330 V_{\text{rms}}$, 100-Hz ac voltage. (b) Two deionized water droplets are dispensed by EWOD actuation by applying $85 V_{\text{rms}}$, 100-Hz ac voltage. (c, d, e) The water droplets are delivered and combined with oil droplets to form DE droplets. (f) The water droplets pull the whole merged water-in-oil DE droplets by EWOD actuation.

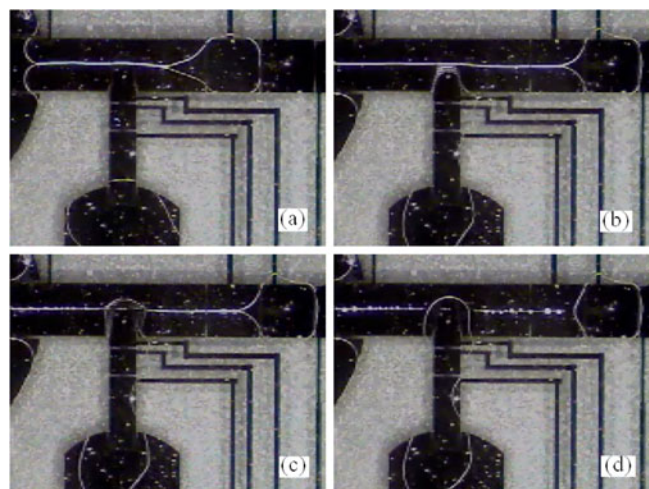


Fig. 11. Breaking the tether with a second water liquid finger. (a) The second liquid (deionized water) in a reservoir. (b) The second liquid finger approaches the "tether." (c) The tether breaks inside the second liquid finger. (d) The entire tether disintegrates into many satellite droplets.

A third approach would be to add the surfactant to the oil to avoid tether formation. We have found that Silwet has little influence on the wetting property of oils, and Silwet-doped oil can be dispensed smoothly. As shown in Fig. 12, when a pure water droplet and a Silwet-doped oil droplet are placed together, an oil-in-water DE droplet can be formed because the Silwet tends to diffuse into the water phase. Unfortunately, the DE droplet formation takes some time because the Silwet diffuses gradually across the interface from the oil phase into the water phase. Using

0.125% [volume-to-volume (v/v)] Silwet-added mineral oil and deionized water droplets, the process takes several minutes. When a 0.5% (v/v) Silwet-modified mineral oil drop is used, the diffusion time is reduced to ~ 10 s.

VI. CONCLUSION

In this paper, we have demonstrated that aqueous and nonaqueous liquid droplets can be dispensed from reservoirs on a microfluidic chip, and the dispensed droplets can then be combined to form oil-in-water-in-air or water-in-oil-in-air DE droplets. In the dispensing process, droplet volume reproducibility has been tested over a range of operational parameters, including applied voltage and the length of the cutting electrode. We find that drop volume variability is mainly caused by variability in the tail volume during pinch-off. When the length of the cutting electrode is increased, volume reproducibility is degraded because longer cutting electrodes reduce the influence of the electrode shape on the radius of curvature in the pinch-off region.

The Gibbs free energy change can be used to test the ability to form stable DE droplets. The result indicates that water-in-oil DE droplets formed through spontaneous emulsification and oil-in-water DE droplets also can be formed by the addition of surfactant and the proper selection of oil. Experimental results show the formation of water-in-oil DE droplets. Using simultaneous DEP and EWOD actuation on a microfluidic chip, dielectric (oil) and conductive (water) droplets have been dispensed, and merged, and the transport of the merged water-in-oil DE droplet has been demonstrated.

The formation of mineral oil-in-Silwet-treated water DE droplets has been demonstrated. We find that a tether

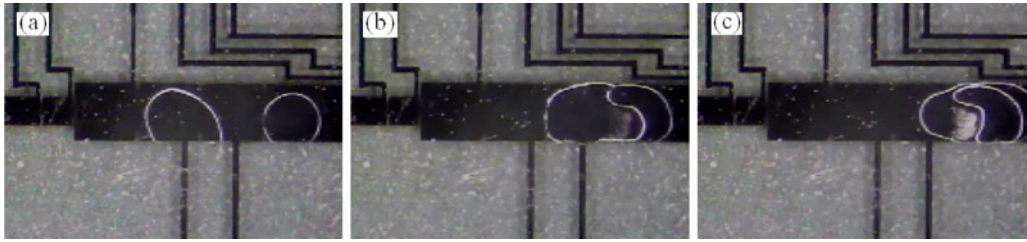


Fig. 12. Formation of an oil-in-water DE droplet. (a) Left: a pure water droplet; right: a 0.125% (v/v) Silwet-added mineral oil droplet. (b) The water droplet is delivered to the oil droplet. (c) Five minutes later, the oil-in-water DE is formed.

is formed during the dispensing of Silwet-treated water. Although the tether can be broken by the disturbance of a second liquid finger, it interferes with the dispensing operation and degrades dispensing reproducibility. Other methods to avoid the tether include taking advantage of the pH effect on Silwet solutions and adding the surfactant to the oil phase. Further effort to develop a more reliable formation method for oil-in-water DE is needed; for example, a surfactant more sensitive to pH might react more quickly so that its recovery of wetting ability (the contact angle reversal) would take much less time. Alternatively, low surface tension water could be dispensed in an oil medium without forming a tether. These schemes will be tested for oil-in-water DE formation.

ACKNOWLEDGMENTS

We thank R. L. Garrell [University of California, Los Angeles (UCLA)] and A. Tucker-Schwartz (UCLA) for valuable discussions about Gibbs free energy theory, and G. Randall (General Atomics) for suggesting the possibility that Silwet can be added to oils. This work was supported by the U.S. Department of Energy Office of Inertial Confinement Fusion under Cooperative Agreement DE-FC52-08NA28302, the University of Rochester, and the New York State Energy Research and Development Authority.

APPENDIX

REQUIREMENTS ON DE DROPLET UNIFORMITY FOR LASER TARGET FABRICATION

The foam shell structure of a concentric laser target is shown in Fig. A.1. The volumes of the inner oil phase V_1 and the outer water phase V_2 are

$$V_1 = \frac{4\pi}{3} R_1^3$$

and

$$V_1 + V_2 = \frac{4\pi}{3} R_2^3 .$$

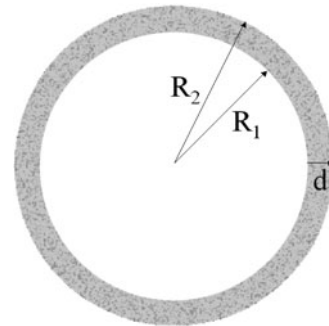


Fig. A.1. The foam shell structure of a concentric laser target.

The shell thickness is

$$d = R_2 - R_1 .$$

Thus, d can be written

$$d = \frac{\left(\frac{3}{\pi}\right)^{1/3} \cdot (V_1 + V_2)^{1/3}}{2^{2/3}} - \frac{\left(\frac{3}{\pi}\right)^{1/3} \cdot V_1^{1/3}}{2^{2/3}} . \tag{A.1}$$

By taking partial derivatives of Eq. (A.1), we obtain an expression for the uncertainty of d in terms of the uncertainties of V_1 and V_2 :

$$\Delta d = \left| \Delta V_1 \cdot \left(\frac{1}{6^{2/3} \pi^{1/3} (V_1 + V_2)^{2/3}} - \frac{1}{6^{2/3} \pi^{1/3} V_1^{2/3}} \right) \right| + \left| \Delta V_2 \cdot \frac{1}{6^{2/3} \pi^{1/3} (V_1 + V_2)^{2/3}} \right| . \tag{A.2}$$

The specified dimensions of an inertial fusion energy (IFE) target are $2R_2 = 4 \pm 0.2$ mm and $d = 289 \pm 20$ μ m. By substituting these values into Eq. (A.2), we can determine wall thickness variation ($\Delta d/d$) in terms of water and oil volume variations ($\Delta V/V$) (refer to Fig. A.2). Different wall thickness variations ($\Delta d/d$) are represented by a set of straight lines in the ($\Delta V_1/V_1$) versus

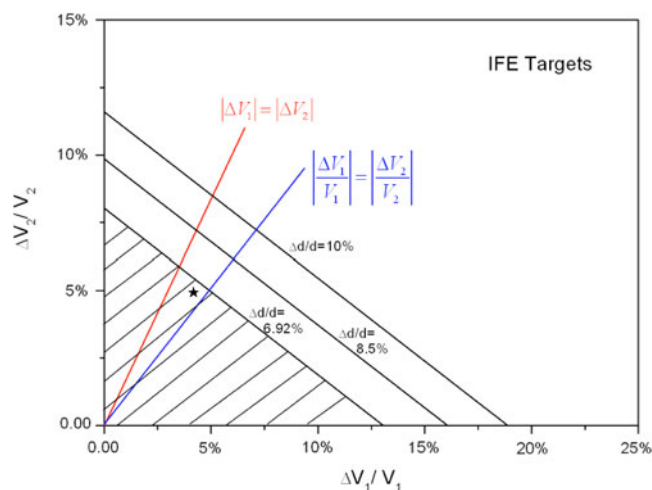


Fig. A.2. Sensitivity analysis of shell wall thickness for IFE target.

($\Delta V_2/V_2$) chart of Fig. A.2. These lines have the same slope, and small ($\Delta d/d$) lines are closer to the original point. The cross-hatched area indicates where the requirement on wall thickness variation is satisfied, i.e., $\Delta d/d < 20/289 = 6.92\%$. For example, if the oil volume variation ($\Delta V_1/V_1$) is 5% and the water volume variation ($\Delta V_2/V_2$) is 4%, the corresponding point indicated by a star in Fig. A.2 locates within the cross-hatched area, which means the wall thickness condition meets the requirement.

The red line in Fig. A.2 represents where the changes of the water and oil phase absolute volumes are the same, and the blue line represents where the relative volume variations of the water and oil phases are the same (color online). Under the condition of identical relative volume variations, $(\Delta V_1/V_1) = (\Delta V_2/V_2)$ must be $< 4.97\%$ to meet the laser target requirement.

REFERENCES

1. S. M. LAMBERT et al., *J. Appl. Poly. Sci.*, **65**, 2111 (1997).

2. R. R. PAGUIO et al., *Mater. Res. Soc. Symp. Proc.*, **901E**, 78 (2006).

3. N. PANNACCI et al., *Phys. Rev. Lett.*, **101**, 164502(4) (2008).

4. A. S. UTADA et al., *Science*, **308**, 537 (2005).

5. S. OKUSHIMA et al., *Langmuir*, **20**, 9905 (2004).

6. R. B. FAIR, *Microfluid. Nanofluid.*, **3**, 245 (2007).

7. T. B. JONES, "On the Relationship of Dielectrophoresis and Electrowetting," *Langmuir*, **18**, 4437 (2002).

8. D. CHATTERJEE et al., *Lab Chip*, **9**, 1219 (2009).

9. M. G. POLLACK et al., *Appl. Phys. Lett.*, **77**, 1725 (2000).

10. S. K. CHO et al., *J. Microelectromech. Syst.*, **12**, 70 (2003).

11. H. REN et al., *Sens. Actuators B*, **98**, 319 (2004).

12. J. BERTHIER et al., *Sens. Actuators A*, **127**, 283 (2006).

13. R. B. FAIR et al., *Technical Digest IEEE International Electron Devices Meeting 2003*, p. 779 (2003).

14. T. B. JONES and M. WASHIZU, *J. Electrostatics*, **37**, 121 (1996).

15. P. R. C. GASCOYNE and J. V. VYKOUKAL, *Proc. IEEE*, **92**, 22 (2004).

16. D. CHATTERJEE et al., *Lab Chip*, **6**, 199 (2006).

17. S. K. FAN et al., *Lab Chip*, **9**, 1236 (2009).

18. T. B. JONES and K. L. WANG, *Langmuir*, **20**, 2813 (2004).

19. K. L. WANG and T. B. JONES, *J. Micromech. Microeng.*, **14**, 761 (2004).

20. M. BIENIA et al., *Physica A*, **339**, 72 (2004).

21. A. STAICU and F. MUGELE, *Phys. Rev. Lett.*, **97**, 167801 (2006).

22. J. RADULOVIC et al., *J. Colloid Interface Sci.*, **332**, 497 (2009).

23. H. KIM et al., *J. Colloid Interface Sci.*, **241**, 509 (2001).